Microfluidic device for chemical and mechanical manipulation of suspended cells

Samaneh Rezvani[1] , **Nan Shi**[2] , **Todd M Squires**[2] **and Christoph F Schmidt**[1]

[1] Faculty of Physics, Third Institute of Physics—Biophysics, University of Göttingen, Göttingen, Germany
[2] Department of Chemical Engineering, University of California, Santa Barbara, CA, United States of America

E-mail: christoph.schmidt@phys.uni-goettingen.de

CrossMark

Abstract

Microfluidic devices have proven to be useful and versatile for cell studies. We here report on a method to adapt microfluidic stickers made from UV-curable optical adhesive with inserted permeable hydrogel membrane micro-windows for mechanical studies of suspended cells. The windows were fabricated by optical projection lithography using scanning confocal microscopy. The device allows us to rapidly exchange embedding medium while observing and probing the cells. We characterize the device and demonstrate the function by exposing cultured fibroblasts to varying osmotic conditions. Cells can be shrunk reversibly under osmotic compression.

Keywords: microfluidic device, photo-polymerization, laser scanning microscopy, suspended cells

S Supplementary material for this article is available online

(Some figures may appear in colour only in the online journal)

Introduction

Microfluidic devices are increasingly used for biophysical experiments, both to study bio-macromolecules, for example in x-ray probes of protein structures [1] or to study cells, for example in optical stretcher experiments designed to investigate cell viscoelasticity [2]. A major advantage of microfluidic devices for cell biophysics is the ability to perform high-resolution optical microscopy in the device, and to achieve high throughput for screening or sorting applications. Fast response of cells can be probed by rapid change of conditions or addition of chemicals [3].

Microfluidic stickers (MFS) are a kind of microfluidic device constructed using UV-curable optical glue. They have been shown to be suitable for culturing cells and tissues [4, 5].

The UV-curable Norland Optical Adhesive NOA-81 is a versatile liquid photopolymer for low-cost microfluidic chip production [6]. Compared to polydimethylsiloxane (PDMS), the more widely used polymer for microfluidics, NOA-81 is entirely transparent and non-scattering in the visible range (refractive index of 1.56). It was developed for fast and transparent bonding of optical components and fiber optics. Additionally, its low auto-fluorescence and high transmission in the near UV range makes it the most promising optical glue among the members of the NOA series [7]. In comparison to PDMS, however, the fluorescence emission of NOA-81 is slightly higher or comparable. Nevertheless, fluorescence cell imaging in micro-devices made of NOA-81 shows a relatively high signal to noise ratio, such that it looks to be an ideal material for live cell imaging (see supplementary figure (stacks.iop.org/JPhysD/51/045403/mmedia)).

NOA-81 shows good chemical resistance to organic solvents, impermeability to oxygen and water vapor, persistence against swelling upon contact with fluids, and stability under

J. Phys. D: Appl. Phys. **51** (2018) 045403

S Rezvani *et al*

surface treatments e.g. by oxygen plasma [6, 8]. A droplet of NOA-81, exposed to UV light, cures within a few seconds to a hard elastic polymer. The peak of sensitivity is around 365 nm, and curing time depends on light intensity and thickness of the liquid layer that has been applied [9]. A further advantage of NOA-81 resin is its high Young's modulus (1 GPa), that allows for channels with large aspect ratios while still maintaining straight rigid walls. After curing, it shows very good adhesion to glass, metals or plastics without swelling or leakage for up to months. In contrast, swelling due to water absorption is still problematic for PDMS-based devices [4].

It is challenging to isolate cells from mechanical perturbations in microfluidic devices while rapidly changing chemical conditions. One method addressing this problem is the insertion of porous windows in microfluidic flow chambers that allow small molecules to rapidly pass between channels without producing substantial hydrodynamic forces [10, 11].

We have here adapted a method to study cells suspended in such a chamber while exposed reversibly to changes of osmotic conditions. We report on the design and fabrication of a versatile microfluidic device with a three-channel configuration that allows us to temporally and spatially control the concentration of osmolytes in the central channel from the side channels. We fabricated MFS of NOA-81 and inserted hydrogel membrane micro-windows (HMM) using scanning confocal microscopy for optical projection lithography.

The microfluidic device was designed such that a rapid exchange of small molecule solutes is possible between the channels while decoupling the rapid fluid flow in the outer channels from the inner channel. The shielding from flow makes it possible to, for instance, study changes in mechanical response of individual cells during rapid changes of solvent conditions without exposing the cells to additional forces from fluid flow. By flushing the side channels, we could also rapidly reverse the medium changes.

Materials and methods

Microfluidic sticker design

A three-channel microfluidic device configuration (figure 1) with a central sample channel located between two parallel outer channels with permeable windows inserted in the walls is an established design to generate concentration gradients across the central channel or introduce symmetrical concentration profiles in the sample channel by diffusion [10]. Windows in the wall are formed by hydrogel membranes. We designed chambers with three channels of 150 μm width and a pair of 50×100 μm^2 rectangular windows on opposing sides of the central channel in 40 to 80 μm high channels (figure 1).

The geometry of the windows plays a role for both, the hydrogel polymerization and for the transport of solutes through the windows. Windows form more uniformly when the channel depth is low and exposure for polymerization is shorter. Diffusive flux through the windows scales with their cross sections and decreases with increased windows thickness.

Height and width of the central channel needs to be adapted to the dimensions of the cells. Typical cell diameters are between 10 and 15 μm, and since cells swell or shrink under different osmolarity, devices with different channel heights were fabricated (ranging from 35 to 70 μm). The width of the side channels was chosen to be 150 μm, and the central channel width was between 150 μm. Using NOA-81, we could fabricate large aspect ratio devices with a length up to 4 cm, without stickers getting torn or deformed while peeling them from the PDMS molds.

### Microfluidic sticker preparation

The preparation of stickers followed an established procedure [4, 5] and is illustrated in figure 2. MFS were fabricated by soft imprint lithography using a negative PDMS stamp, UV-polymerizable resin NOA-81 (Norland Products Inc., Cranbury, NJ, USA), and a flat PDMS mold. The negative PDMS stamp was made by replica molding of a SU-8 photoresist mold produced by standard photo-lithography (using a patterned chromium on glass mask). A drop of UV curable resin NOA-81 (500–700 μl) was poured on a flat PDMS mold (figure 2) and sandwiched with the structured PDMS stamp. After 2–3 min of UV exposure (365 nm), the PDMS stamp was peeled off and after punching inlet/outlet holes at the end of the channels, replaced with a cover slip cleaned with isopropanol (IPA). The flat PDMS mold together with the NOA sticker on the coverslip, was exposed to UV light for the second time (2 min) through the flat PDMS. In this step, NOA further polymerizes so that the PDMS mold could be detached from the flat PDMS substrate, while the sticker remains tightly bound to the coverslip. The NOA sticker attached to the cover slip was flipped over and exposed to UV exposure for the last time (2 min). UV radiation time was optimized based on the aspect ratio and geometry of the channels. After this step, the inlet/outlet connections were fixed with small acrylic rings and a drop of 5 min epoxy glue to the sticker.

Photo-polymerization of HMM

Photo-polymerization is a relatively new method of light-based lithography. Photo-initiated polymerization has become a popular technique for hydrogel formation *in situ*, owing to its adjustable temporal and spatial resolution [12]. Minimum feature resolution, depth of focus (DOF), photo-initiator, hydrogel precursor response, light source, oxygen contribution and sample thickness are the key parameters in such photo-lithography process.

The smallest feature size of a given pattern that the projection system can print faithfully is proportional to λ/NA, where λ is the illumination wavelength and NA the numerical aperture of the projection lens.

DOF scales like $\lambda/(\mathrm{NA})^2$, and determines the focus error that still gives an acceptable lithographic result. It limits how much the fabrication plane can be displaced while resulting structural features remain sufficiently sharp. High resolution and large DOF are mutually exclusive, creating an
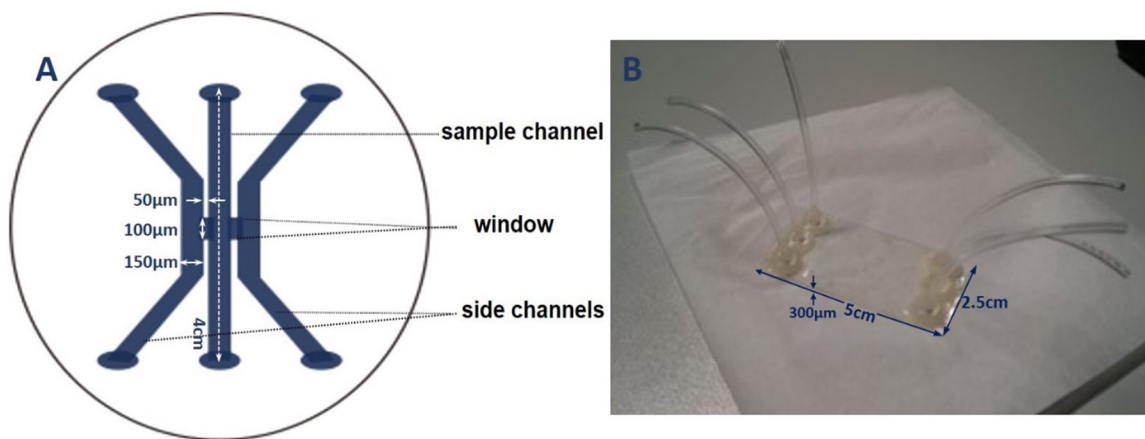
Figure 1. Schematic design (not to scale) and photograph of the microfluidic sticker based chamber. Two side channels are connected to the sample channel in the middle via open windows in the walls. All three channels are designed with the same width of 150 μm, with walls of 50 μm between channels. Windows are 100×50 μm^2. (A) Schematic design on a 2 inch silicon wafer. (B) Sticker sealed onto a cover slip with tubes glued to inlet/outlet ports. Thickness of the sticker without cover slip is <200 μm.

optimization problem. Since in our case structural details are not extremely fine, but the window height is large, we opted for low resolution and large DOF using a low NA objective (NA = 0.45).

Oxygen is a major inhibitor of photo-polymerization. Since the NOA-81 sticker and the glass cover slip are both impermeable to oxygen, long UV exposure was not an issue in our fabrication process [13].

We used poly-ethylene-glycol-diacrylate (PEG-DA) as material for photo-polymerization with 405 nm UV light. Chemical composition, concentration (volume ratio) of photo-initiator and intensity of UV light will change the gelation time [12, 14, 15]. Fabrication of hydrogel membrane micro windows (HMMs) in a microfluidic device, has been introduced previously [10]. Here, we essentially followed the published procedure using UV photo-polymerization to insert HMMs in the gaps left in NOA walls (windows in figure 1) of the channels of our microfluidic sticker.

First, we prepared an aqueous hydrogel precursor solution made of 95% v/v polyethylene glycol diacrylate (PEG-DA, $n = 400$, 01871-250 Polysciences Inc.) and 5% v/v photo-initiator (2-hydroxy-2-methylpropiophenone, 405655, Sigma-Aldrich). Then, the whole chamber was filled with the hydrogel solution. UV induced polymerization of PEG-DA was performed with a Leica TCSSP5 scanning confocal microscope, defining a scanning pattern such that windows were fabricated in the appropriate size and locations.

The intensity provided by the 405 nm diode laser in the focal spot of the 10x objective (NA = 0.45), was 400–500 mW cm^{-2} (50 mW of laser power passing through the objective). The sample was mounted on a motorized stage while the objective was focused on the mid plane of the channels. As shown in figure 3, the scanning mirror was programmed to sweep a rectangular region of interest (ROI) of 70×130 μm^2 that was positioned to cover the gap in the chamber wall (extending slightly further to anchor the edge of the 50×100 μm^2 windows). 1–3 s of illumination with 95% of maximum intensity was enough to polymerize the HMMs to the full height of 40 to 80 μm deep channels. Immediate rinsing of

uncured precursor solution, after illumination was important. This was done by 10–20 min continuous wash with water.

Cell culture

In this work, we used NIH 3T3-fibroblasts (mouse embryonic fibroblasts), which are naturally adherent cells (DSMZ, Braunschweig, Germany). Cells were cultured in Dulbecco's modified Eagle's medium (DMEM) (D6429, Sigma-Aldrich, St. Louis, MO, USA) with 10% fetal bovine serum (FBS, F0244, Sigma-Aldrich) and 1% penicillin-streptomycin (17-602E, Lonza, Basel, Switzerland) in 75 cm^2 culture flasks (83.1813, Saarstedt AG, Nümbrecht, Germany) at 37 °C and 5% CO$_2$. Cells were grown up to roughly 80% confluency and passaged into new culture flasks using 0.05% trypsin (59417C, Sigma) every 2–3 d with a density of ~150 000 cells per flask.

Suspension of cells in the microfluidic device

Bio-compatibility

Neither PEG hydrogels, nor NOA-81 are poisonous to the cells. Biocompatibility of microfluidic devices made of NOA-81 has been reported previously [5]. MFS have also been used for tissue culturing [4]. PEG-DA hydrogels have been explored in the form of 2D substrates, scaffolds or 3D capsules for cells and tissue engineering. The materials was found to be inert and non-toxic to cells [15–19]. To prevent cell adhesion to the channel walls, we here additionally silane coat the channel surfaces using Dichloro-dimethyl-silane (DDS) vapor, which is not toxic for cells. This silane compound in liquid form has been used successfully to coat glass cover slips for suspended cell assays in previous work [20]. To confirm cell viability in the MFS, we repeatedly measured the mechanical properties of cells suspended in the device, such as stiffness, using dual optical traps, for more than 2 h and found no significant changes (~6% variation) in the results in this period. The supplementary figure shows fluorescent labelled 3T3 fibroblast cells suspended in such a micro-device.
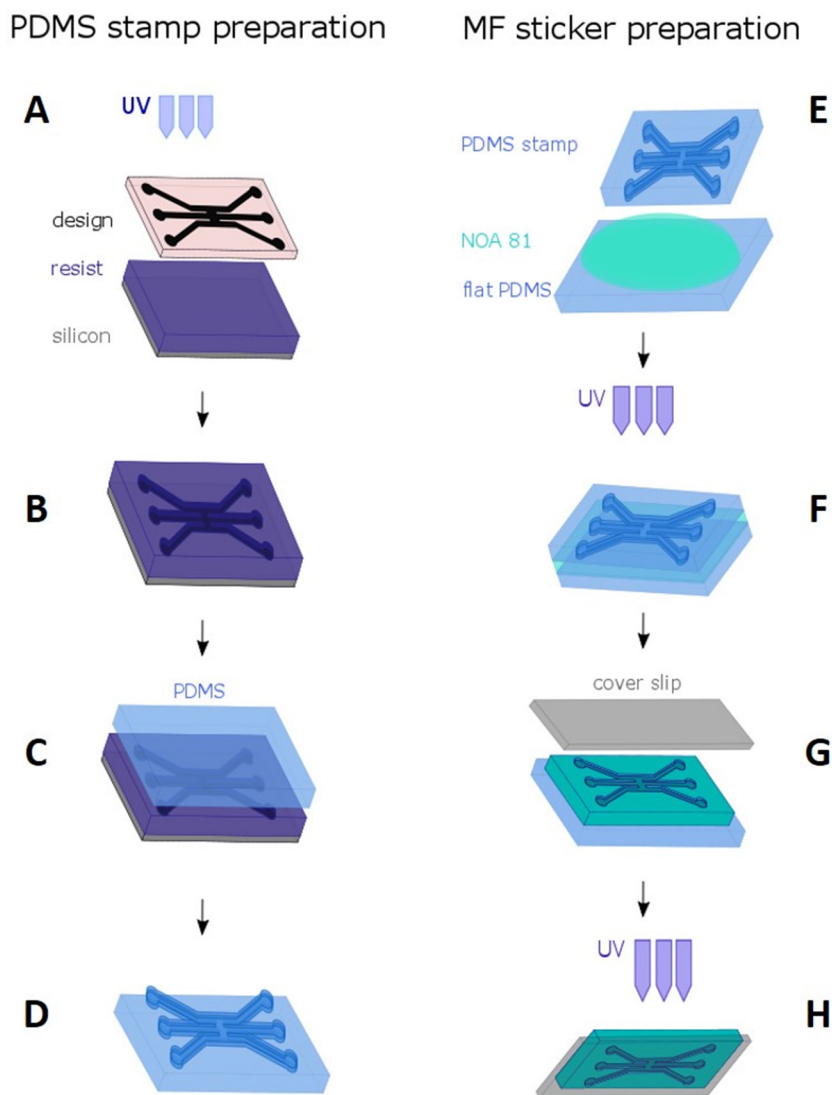
Figure 2. Sticker preparation. MFS were fabricated from UV-curable optical adhesive NOA-81 using a PDMS stamp and then assembled on a glass cover slip. (A)–(D) PDMS stamp preparation. (E)–(H) Microfluidic sticker construction. (A) Patterning of SU-8 photo-resist on a silicon wafer using a chromium-coated glass mask. (B) Positive master mold of photoresist on silicon with desired pattern and geometry. (C) PDMS solution cast onto the master mold to produce negative stamp. (D) PDMS stamp is peeled off from the master mold. (E) Liquid NOA-81 is sandwiched between the stamp and a flat PDMS mold to create the sticker. (F) PDMS-NOA-PDMS sandwich is exposed to 365 nm UV. (G) PDMS stamp is peeled off from the sticker and replaced by a pre-cleaned cover slip ($24 \times 50\,\text{mm}^2$). (H) Flat PDMS support is peeled off and sticker is again exposed to UV. 365 nm is the peak sensitivity of NOA-81 and exposure time, depending on radiation intensity, was varied between 2 to 4 min.

Surface passivation

Surface passivation of the inner surfaces of the device is crucial to prevent adhesion of cells. Accumulation of cells can rapidly clog the channels when left untreated. Polymerized NOA-81 produces hydrophilic surfaces [8]. To prevent cell adhesion, we rendered the glass and NOA surfaces hydrophobic by vapor silanization with dimethyldichlorosilane (DDS).

In order to not interfere with the adhesion of the sticker to the glass substrate and to obtain well sealed chambers, silanization has to be done on assembled devices. We used negative pressure to flow silane vapour through assembeled channels for about 10 min. This treatment kept chambers non-adhesive for cells for at least a few weeks.

Hydrophobicity of NOA devices using vapor silanization has been reported to last for 40 d [6]. To perform the silanization, a sticker with open inlet/outlet holes was faced down on top of a small container of 5% DDS-in-Heptane solution (85126, Sigma-Aldrich, Germany) and placed into a desiccator. Evacuating the desiccator vaporizes the DDS solution. The vapor was then sucked through the central channel using a syringe.

Recycling the MFS

Our microfluidic devices could be re-used multiple times, as long as they were properly maintained. Since NOA is rather rigid with very good adhesion to glass after UV curing, we did not experience any swelling or leakage of
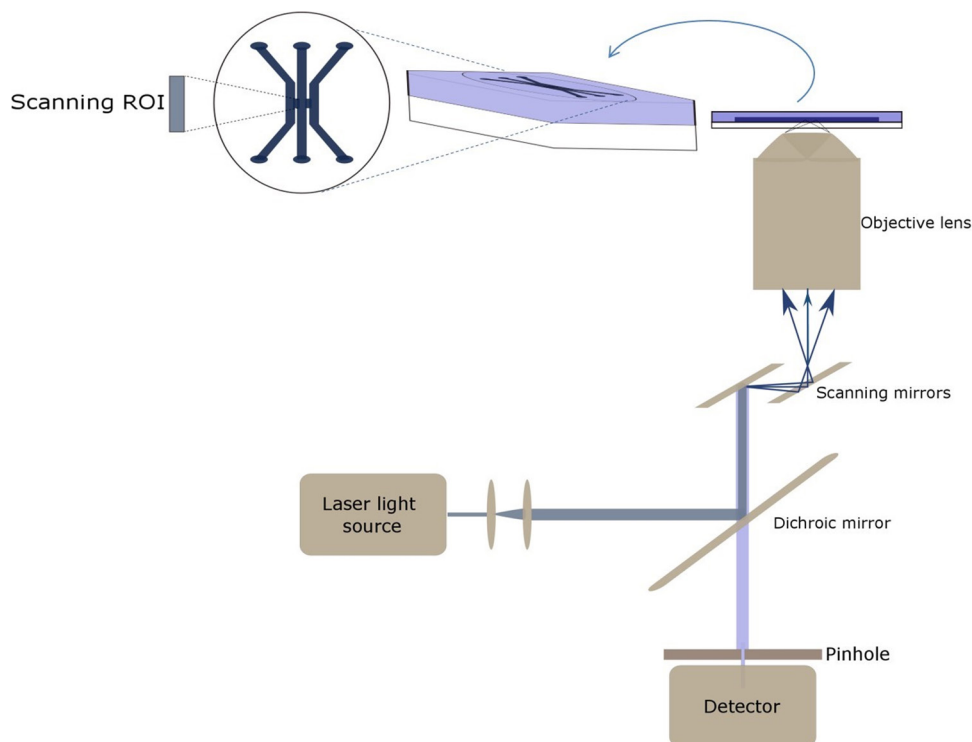
Figure 3. Photo-polymerization of permeable hydrogel micro-membrane windows using laser scanning confocal microscopy. A 405 nm diode laser was focused by a 10× air objective into the mid plane of the microfluidic sticker, which was pre-filled with photo-curable PEG-DA solution. The confocal scanning mirrors are used to scan a rectangular pattern covering the open windows in the NOA walls of the sticker (ROI). Laser intensity in the focal spot was 400–500 mW cm^{-2}. Scanning for 1–3 s scanning was sufficient to polymerize an HMM window up to 80 μm high.

the device even when the channels were kept wet for a few weeks. Bacterial growth, however, needed to be avoided in all three channels. Due to the presence of the culture medium for cells, bacterial growth is expected and indeed was observed. To clean the chamber before and after use, micro-channels were washed and filled with IPA for 10–20 min. Then, they were washed with distilled water for the same time. After cleaning, the devices were ready to re-use and can be filled with the cell medium. Moreover, we used micro filters (0.2 μm pore size) for all solutions before infusing into channels.

Fluid flow control

In order to drive and control flow through the microfluidic channels, we used positive pressure provided by a compressed-air source, following established procedures [21]. In principle, each of the channels can be fed from an individual reservoir. With the aid of a pressure regulator, channels were filled by pressurizing solutions from sealed centrifuge tubes connected to each of the three channels.

Once inlet of the central (sample) channel was closed off, the pressure gradient along this channel largely vanished. However, due to the presence of the permeable windows between channels, flow can occur through the windows from the pressurized side channels. If flow in the side channels is kept running, flow is driven through the membrane windows due to the pressure gradient (trans-membrane flow). However, when the outlet of the central channel is also closed, pressure

equilibrates rapidly and only diffusion through the HMMs will occur [11].

Results

Hydrogel membrane fabrication using confocal microscopy

Confocal scanning hydrogel fabrication is a relatively simple and rapid method for 3D printing of structures in microfluidic chambers. We here used single-plane laser scanning hydrogel fabrication with a simple straight-line pattern design in combination with UV-polymerizable pre-cursor fluids. In principle, one can also print more complicated patterns as well as performing multi-layer and multi-step fabrication by scanning confocal.

We wrote the patterns with a focused 405 nm UV laser (see methods). Up to 80 μm high hydrogel windows could be printed with 2 s of scanning with the UV laser, shown in figures 4(A)–(C). This improves the previously used method, where 500 ms of UV illumination through a photo mask from a mercury lamp with 30 mW cm^{-2} intensity was used for window fabrication in a 10 μm high device [10].

HMM thickness, pore size and exposure time

HMM thickness and its pore size will change with the duration of UV exposure and laser power. Longer UV exposure results in wider, more bulging membranes and smaller pores. The same is true for increased light intensity. The permeability of

J. Phys. D: Appl. Phys. **51** (2018) 045403

S Rezvani *et al*
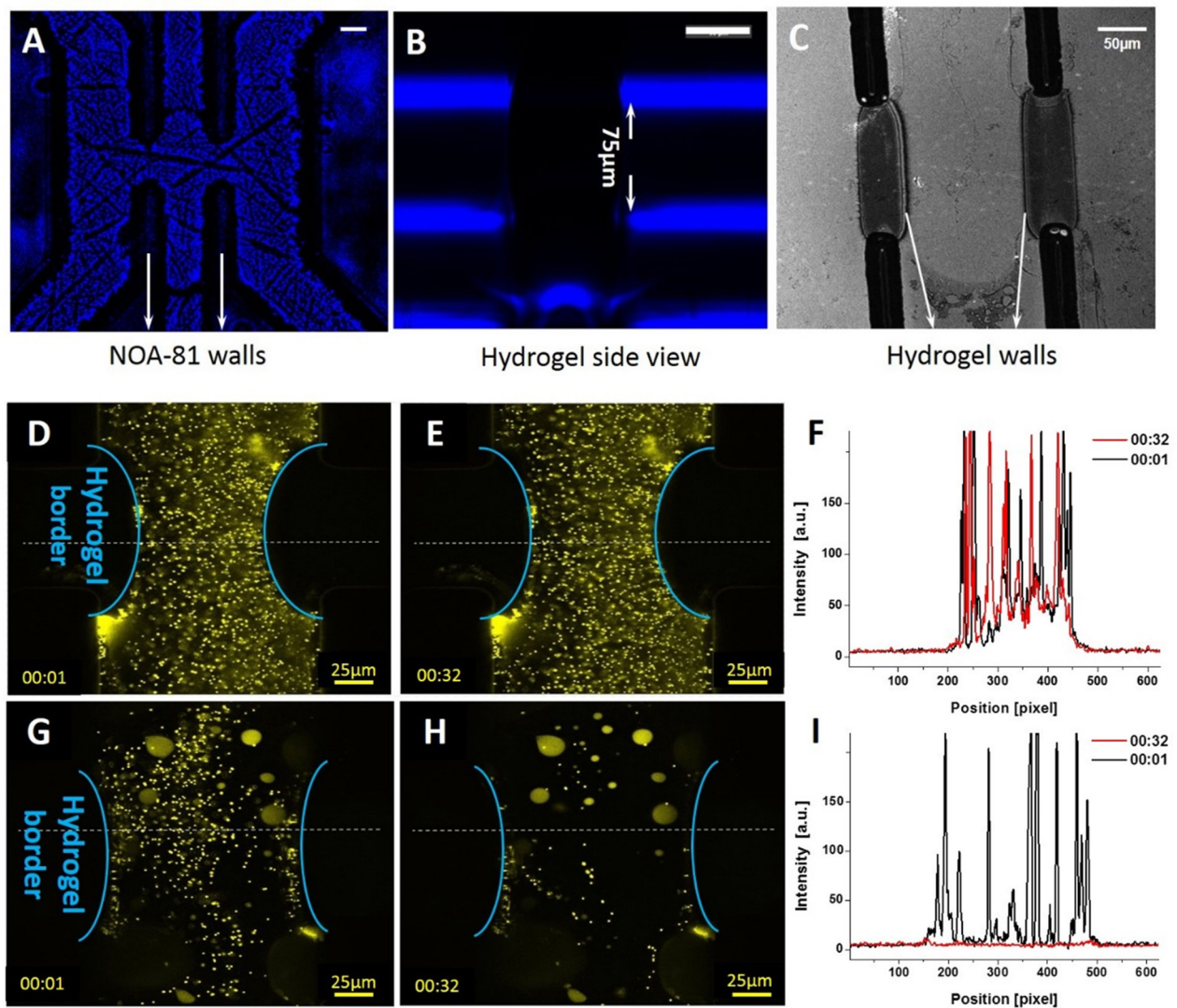
Figure 4. Photo polymerization of HMM windows inside the microfluidic chamber. Top panel: (A) chamber filled with uncured PEG-DA. NOA-81 walls between outer and inner channel are shown. (B) Side view of completed 75 μm high HMM window. (C) Top view of HMM windows anchored to NOA walls. Up to 80 μm high HMM windows with straight walls were produced, while the laser was scanning the rectangular gaps in the NOA walls in the mid plane of the filled chamber (top panel scale bars: 50 μm). Middle panel: thick HMM windows fabricated with long UV exposure. 2595 ms UV exposure resulted in thick HMM windows (inner edges marked in blue). (D) Initial distribution of 1 μm fluorescent beads in the sample channel when buffer starts flowing through side channels. (E) Distribution of tracer beads with no change in concentration after 32 s of flowing 2 mM solution through the side channels (scale bar: 25 μm). (F) Fluorescence intensity profiles along dashed lines marked in (D) and (E) at the beginning, $t = 1$ s, is compared to intensity at $t = 32$ s after buffer solution starts flowing through side channels. Bottom panel: thin hydrogel HMM windows fabricated with short UV exposure. 1500 ms UV exposure forms thin hydrogel windows (inner edge marked in blue). (G) Initial distribution of 1 μm fluorescent beads, in the sample channel when the buffer starts flowing through side channels and central channel is closed. (H) Distribution of tracer beads in sample channel changed after 32 s when the buffer passed through the thinner HMM windows (scale bar: 25 μm). (I) Fluorescence intensity profiles along dashed lines marked in G and H at the beginning, $t = 1$ s, compare to intensity at $t = 32$ s after buffer solution started flowing through side channels.

the HMM for macromolecules (i.e. sugars, drugs or proteins) depends on these two parameters.

We tested the permeability of our laser-fabricated HMMs, in two separate ways. First as shown in figures 4(D)–(I), we flowed fluorescent micro-spheres into the central (sample) channel and ran solutions containing buffer through the outer (side) channels and followed permeability of HMMs by watching the displacement of the particles.

Second, using live cell imaging, we introduced suspended 3T3-fibroblasts cells to the sample channel and flowed a solution of sorbitol (5–10%) in the outer channels while the central channel was closed on both ends. Diffusion of sugar through HMMs changed the osmotic pressure differences across the cell membrane and resulted in changes in cell size (figure 6).

Hydrogel membrane pores are small enough to effectively decouple fluid flow in the side channels from flow in the central channel, but the pores are large enough to allow for rapid diffusion of solute/solvent molecules. Longer UV exposure time results in wider HMMs with smaller pores

J. Phys. D: Appl. Phys. **51** (2018) 045403

S Rezvani *et al*
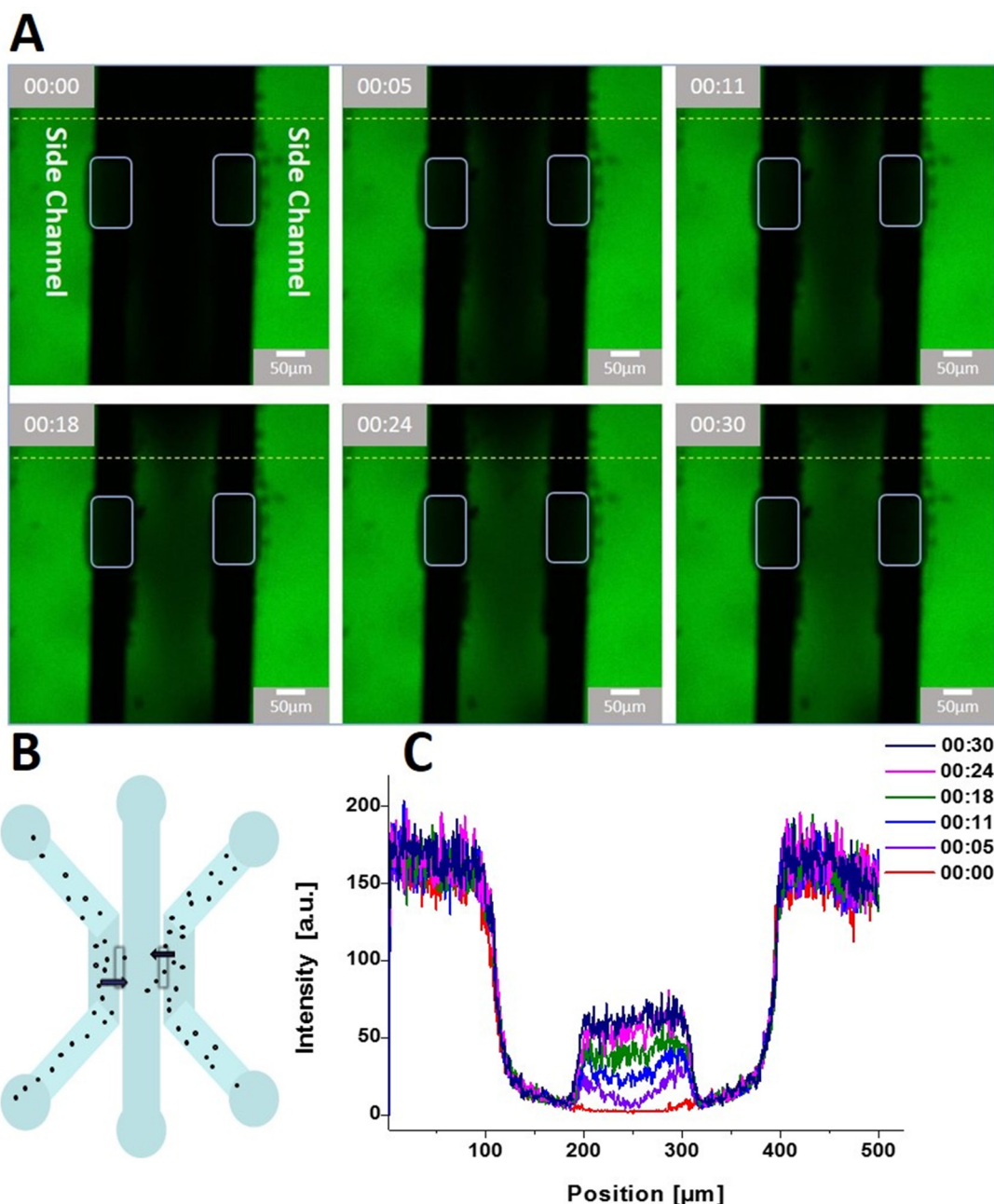
Figure 5. (A) Diffusion of fluorescein dye through hydrogel micro-windows. Concentration pattern of fluorescein in the central channel after diffusion from the side channels through the (closed-) central channel over time. (B) Schematic view of molecular diffusion through HMM windows. (C) Fluorescence intensity profiles along the dashed lines in (A). Fluorescein solution with high intensity is kept running through side channels. The initial intensity in the central channel was zero. Snapshots were recorded at indicated time after filling the side channels with dye. Diffusion through HMM windows increased the fluorescence intensity in the central channel. HMM windows were $50 \times 100 \ \mu m^2$, all three channels are 150 μm wide, and walls were 40 μm high.

and therefore less trans-membrane flow is expected [10]. The practical parameter to vary in order to control the thickness of the windows was the exposure time during the scan. Increasing the exposure time from 1.5 s to 2.6 s increased the maximal thickness of the 40 μm high hydrogel window from ~100 μm to ~150 μm when all other parameters such as volume fraction of photoinitiator (5% v/v), laser intensity (500 mW cm^{-2}) and the scanning area (70 $\times$ 130 μm^2) were kept constant.

Figures 4(D)–(F) shows negligible flow through the HMMs produced with ~2.6 s exposure. Membrane windows turned

out to be thick and bulged out in the middle. For this experiment, a 2 mM buffer was flown in the side channels, while the central channel contained 1 μm diameter fluorescent beads. The distribution of beads was followed by scanning the fluorescence intensity in the middle of the windows. Within 32 s no difference in the distribution of the micro beads could be observed (figure 4, supplementary movie S1).

When UV exposure time was decreased to ~1.5 s (figures 4(G)—(I) and S2), windows were thinner and buffer flow through the windows displaced the micro particles with all other conditions unchanged.
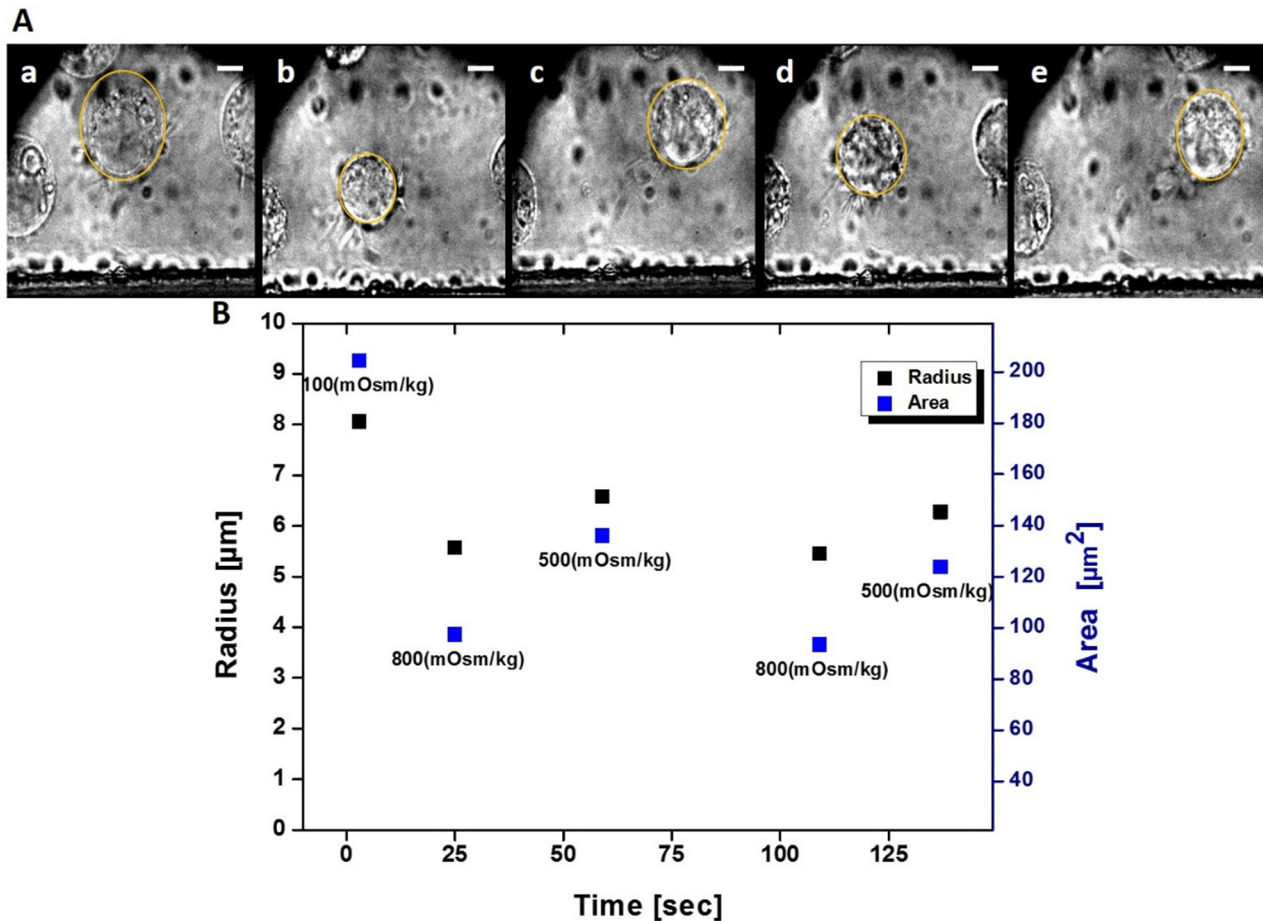
Figure 6. (A) Cell in rapidly changing osmotic conditions. Rapid switching of the solution flowing through side channels changes osmotic conditions in the central channel. Single cells can be identified and followed over time. 3T3 fibroblast cells in the sample channel swell or shrink corresponding to the osmotic shocks. The solution pumped through the side channels changed from hypo- to hyper-tonic with about 30 to 40 s dwell times. Side solution were changed from (a) hypotonic 100 mOsm kg^{-1} to (b) hypertonic 800 mOsm kg^{-1}, followed by (c) less hypertonic 500 mOsm kg^{-1}, then (d) back again to 800 and finally to (e) 500 mOsm kg^{-1}. The cell circumference was fit by eye (scale bars: 5 μm). (B) Size changes of 3T3 fibroblast cell under rapid change of osmotic conditions. Rapid exchange of the side solution made the cell in the central channel swell or shrink. Cross-sectional area (blue) and radius (black) of the cell, fit by eye, in the central channel of the microfluidic chamber versus time. According to the solution running through the side channels, the cell did shrink or swell. Osmolarity of the side-channel solutions in each step is indicated.

Diffusion through HMM

Diffusion time τ_D over a distance L for a solute or molecule with diffusivity D scales like $\tau_D \sim L^2/D$. Typical diffusivity for small organic molecules like glucose and sucrose, or small solute molecules like NaCl in water is on the order of $D \sim 10 \ \mu m^2 \ s^{-1}$ [22]. Therefore, the time for diffusive delivery for such molecules over 100 μm, will be τ_D ~10 s. According to [10], the time needed for diffusing into a micro-channel through a HMM becomes $\tau_D \sim (2\omega_m + \omega_s)^2/\pi^2 D$, where ω_s is the width of sample channel, ω_m the thickness of the membrane and D is the diffusion coefficient of molecules passing through.

Experimentally, we investigated the diffusion of fluorescein sodium salt through our laser fabricated hydrogel membrane windows. In this experiment, the central channels was closed at both ends, such that flow through the HMMs was suppressed. The results are shown in figure 5. Figure 5(A) shows snapshots after consecutive time intervals of ~5 s. Figure 5(B) shows a fluorescence intensity profile along the dotted line in

5(A), developing in time as the dye concentration spreads in the central channel (movies S3 and S4).

Considering the dimensions of the device (150 μm sample channel and ~50 μm thick HMM windows) and diffusion from both of the side channels to the central channel, the results are consistent with the theoretical estimate of $\tau_D < 10$ s.

Step-wise and reversed osmotic pressure changes

By rapid exchange of the medium flowing in the side channels, it is possible to switch back and forth between different medium conditions within a few seconds. The speed of this process is limited by the diffusion through the membrane windows. When flow is maintained, solutes will, of course, continue to diffuse in or out of the central channel until complete equilibrium between channels is eventually reached.

We performed experiments under varying osmotic conditions for suspended fibroblasts loaded into the central channel with waiting periods of 30–40 s. Channels had been filled with the cell culture medium, resulting in an isotonic environment

J. Phys. D: Appl. Phys. **51** (2018) 045403

S Rezvani *et al*

for the cells. Then, they were exposed to rapid exchanges of medium from extreme hypotonic (100 mOsm kg^{-1}) to hypertonic media (500 mOsm kg^{-1} and 800 mOsm kg^{-1}) and back again. Figure 6 show how radius and cross-section area of a cell altered in response to these medium changes (S5).

Conclusions

We have described the fabrication and application of a three-channel microfluidic device with integrated hydrogel micromembranes (HMMs) for suspended cell studies.

We demonstrated how photo-polymerization of the hydrogel windows can be performed using a standard scanning confocal microscope. We applied the device to study rapid osmotic swelling and shrinking of fibroblast cells while observing them with a high-magnification microscope.

This works opens a new window to efficient studies of single-cell response to mechanical manipulations, as well as biochemical perturbations and osmotic changes.

Acknowledgments

ORCID iDs

Samaneh Rezvani ⓘ https://orcid.org/0000-0002-5358-0710

References

[1] Saldanha O, Brennich M E, Burghammer M, Herrmann H and Köster S 2016 The filament forming reactions of vimentin tetramers studied in a serial-inlet microflow device by small angle x-ray scattering *Biomicrofluidics* **10** 24108

[2] Chan C J *et al* 2015 Myosin II activity softens cells in suspension *Biophys. J.* **108** 1856–69

[3] Velve-Casquillas G, Le Berre M, Piel M and Tran P T 2010 Microfluidic tools for cell biological research *Nano Today* **5** 28–47

[4] Morel M, Bartolo D, Galas J-C, Dahan M and Studer V 2009 Microfluidic stickers for cell- and tissue-based assays in microchannels *Lab Chip* **9** 1011–3

[5] Bartolo D, Degre G, Nghe P and Studer V 2008 Microfluidic stickers *Lab Chip* **8** 274–9

[6] Wägli P, Homsy A and Rooij N F 2010 Norland optical adhesive (NOA81) microchannels with adjustable surface properties and high chemical resistance against IR-transparent organic solvents *Proc. Eng.* **5** 460–3

[7] Wägli P, Guélat B, Homsy A and De Rooij N 2010 Microfluidic devices made of UV-curable glue (NOA81) for fluorescence detection based applications *Int. Conf. on Miniaturized Systems for Chemistry and Life Sciences* pp 1937–9

[8] Dupont E P, Luisier R and Gijs M A M 2010 NOA 63 as a UV-curable material for fabrication of microfluidic channels with native hydrophilicity *Microelectron. Eng.* **87** 1253–5

[9] www.norlandprod.com/adhesives/noa (Norland Optical Adhesive 81)

[10] Paustian J S, Azevedo R N, Lundin S-T B, Gilkey M J and Squires T M 2013 Microfluidic microdialysis: spatiotemporal control over solution microenvironments using integrated hydrogel membrane microwindows *Phys. Rev.* X **3** 13

[11] Paustian J S *et al* 2015 Direct measurements of colloidal solvophoresis under imposed solvent and solute gradients *Langmuir* **31** 4402–10

[12] Fairbanks B D, Schwartz M P, Bowman C N and Anseth K S 2009 Photoinitiated polymerization of PEG-diacrylate with lithium phenyl-2,4,6-trimethylbenzoylphosphinate: polymerization rate and cytocompatibility *Biomaterials* **30** 6702–7

[13] Belon C, Allonas X, Croutxé-barghorn C and Lalevée J 2010 Overcoming the oxygen inhibition in the photopolymerization of acrylates: a study of the beneficial effect of triphenylphosphine *J. Polym. Sci.* A **48** 2462–9

[14] Arcaute K, Mann B K and Wicker R B 2010 Fabrication of off-the-shelf multilumen poly (ethylene glycol) nerve guidance conduits using stereolithography *Tissue Eng.* C **17** 27–38

[15] Thomas A M and Shea L D 2014 Cryotemplation for the rapid fabrication of porous, patternable photopolymerized hydrogels *J. Mater. Chem.* B **2** 4521–30

[16] Caliari S R and Burdick J A 2016 A practical guide to hydrogels for cell culture *Nat. Methods* **13** 405–14

[17] Durst C A, Cuchiara M P, Mansfield E G, West J L and Grande-Allen K J 2011 Flexural characterization of cell encapsulated PEGDA hydrogels with applications for tissue engineered heart valves *Acta Biomater.* **7** 2467–76

[18] Klein F *et al* 2011 Two-component polymer scaffolds for controlled three-dimensional cell culture *Adv. Mater.* **23** 1341–5

[19] Arcaute K, Mann B and Wicker R 2010 Stereolithography of spatially controlled multi-material bioactive poly(ethylene glycol) scaffolds *Acta Biomater.* **6** 1047–54

[20] Schlosser F, Rehfeldt F and Schmidt C F 2015 Force fluctuations in three-dimensional suspended fibroblasts *Phil. Trans. R. Soc.* B **370** 20140028

[21] Bong K W *et al* 2011 Compressed-air flow control system *Lab Chip* **11** 743–7

[22] Hannoun B J M and Stephanopoulos G 1986 Diffusion coefficients of glucose and ethanol in cell-free and cell-occupied calcium alginate membranes *Biotechnol. Bioeng.* **28** 829–35